Tests Of Er-4 And Etgar-3 Facilities At Ben-Gurion University

Author(s): H. Branover, A. El-Boher, SH. Lessin, and M. Petrick

Session Name: Closed-Cycle/Disk Generators

SEAM: 24 (1986)

SEAM EDX URL: https://edx.netl.doe.gov/dataset/seam-24

EDX Paper ID: 1158

24TH SYMPOSIUM
ON ENGINEERING ASPECTS OF
MAGNETOHYDRODYNAMICS

TESTS OF ER-4 AND ETGAR-3 FACILITIES AT BEN GURION UNIVERSITY

H. BRANOVER, A. EL-BOHER, SH. LESSIN
BEN GURION UNIVERSITY
BEER-SHEVA, ISRAEL

AND

M. PETRICK
ARGONNE NATIONAL LABORATORY
ARGONNE, ILLINOIS

BUTTE, MONTANA
JUNE 24-27, 1986

TESTING OF OMACON-TYPE LMMHD POWER CONVERSION SYSTEMS

* Optimized Magnetohydrodynamic Conversion System (OMACON)

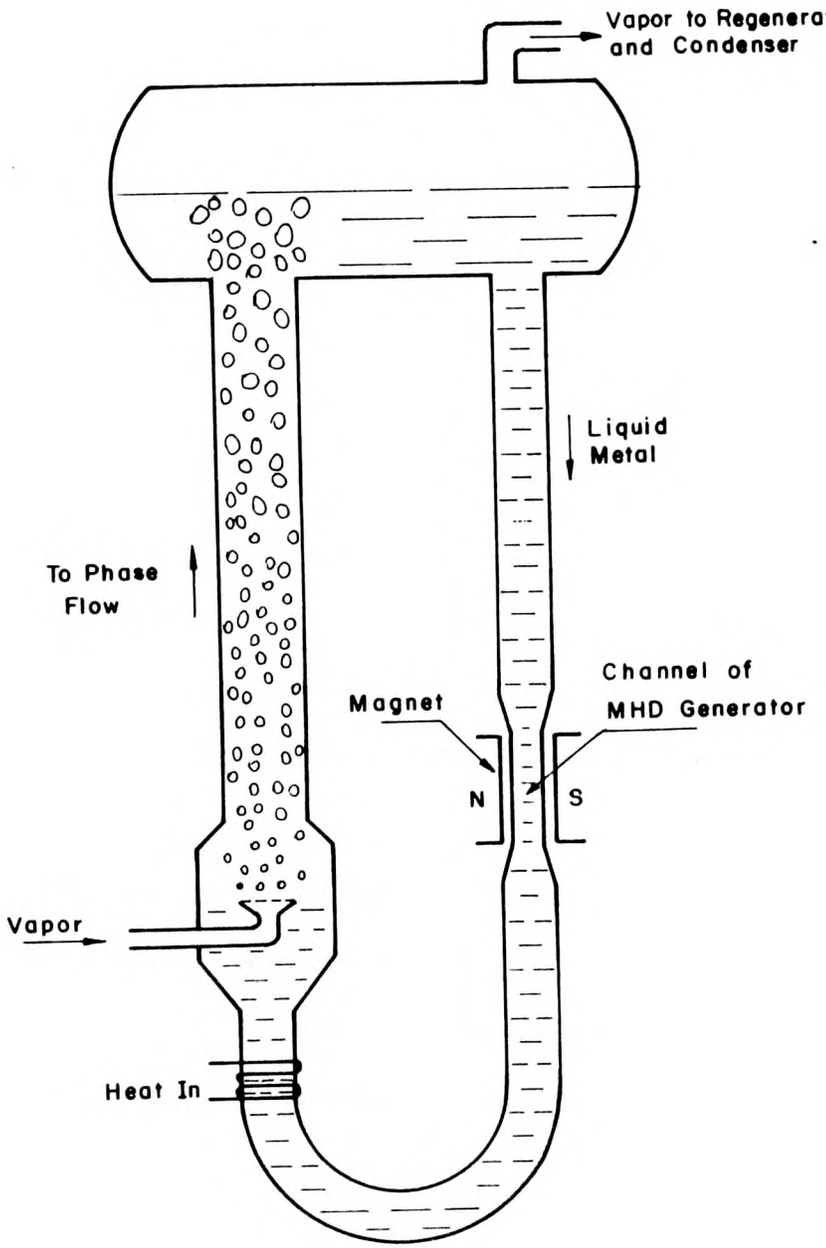

Fig. 1 Schematic of optimized magnetohydrodynamic conversion system (OMACON)

GOALS

* **Verification of computer-code assumptions**
  - Flow phenomena
    - Flow pattern
    - Void fraction and slip
    - Two-phase flow friction
    - Separation
  - MHD Generator performance

* **Assessment of computer code simulation**

* **General observations**
  - Start-up and shut-down procedures
  - Continuous system and components performance
  - Maintenance and failure analysis

* **Advantages of the OMACON system**

- Eliminate the critical, high-loss components in the two-phase flow generator MHD system, namely, the two-phase nozzle, separator, and diffuser.
- Facilitate ultra-simple start-up, operation and shut-down.
- Eliminate two-phase flow limitation of MHD generator performance and hence overall system performance.
- An 80-85% efficient single-phase MHD generator can be achieved and designed with confidence from the data base that exists today.
- The single-phase flow through the MHD generator facilitates the use of low-field, low-cost magnets.
- The high electrical conductivity single-phase flow through the generator makes possible the use of an ac induction generator to produce ac power directly, eliminating the inverter and replacing the magnet with a conventional type of coil system found in electrical motors.
- The overall system can be designed to have low kinetic energy (frictional) losses, thus maximising performance potential.
- Since the fluid passing through the generator is single-phase and at constant velocity, a high electrical efficiency generator design can be utilized.
- Electrical parameter fluctuations caused by two-phase flow instabilities in the generator are eliminated.
- The system can be operated as a Rankine or Brayton cycle and be readily adapted to various temperature ranges applications by proper selection of the working fluids.

* Multistage OMACON system

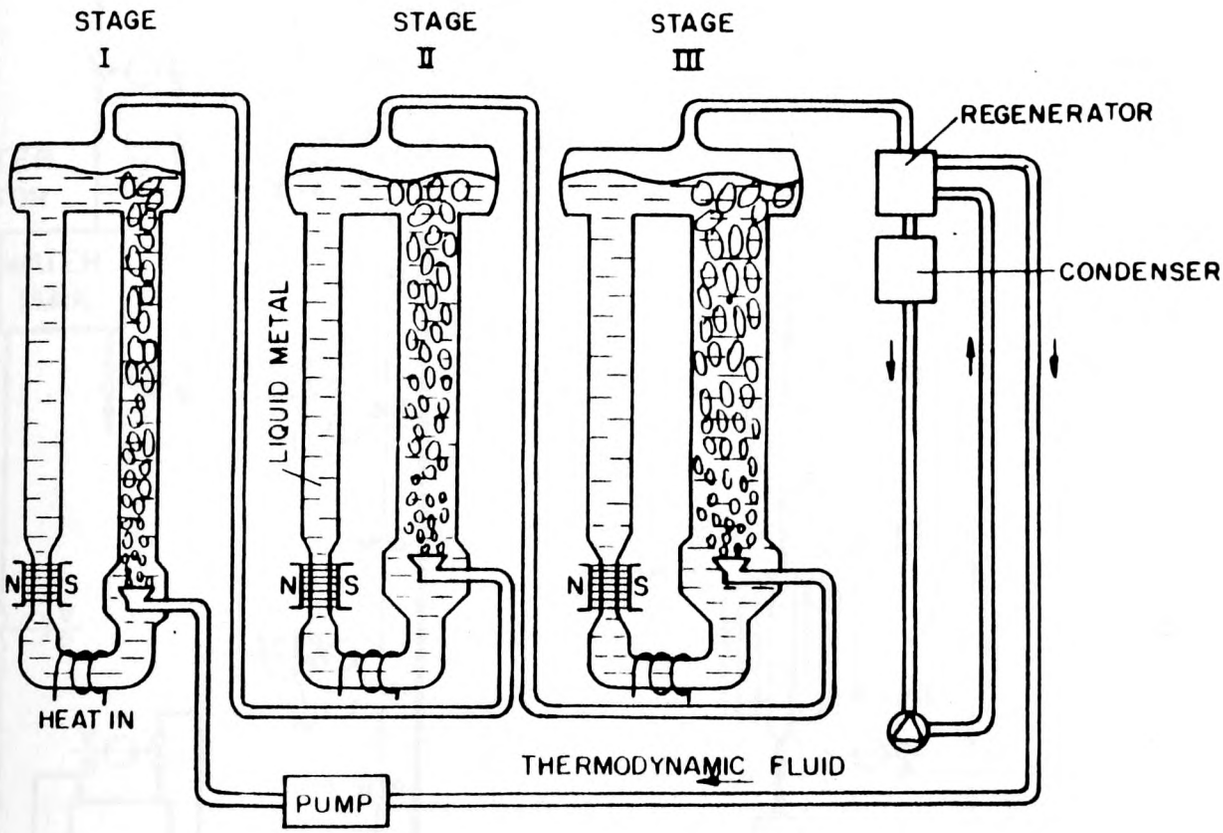

Fig. 2 Schematic of multistage OMACON system

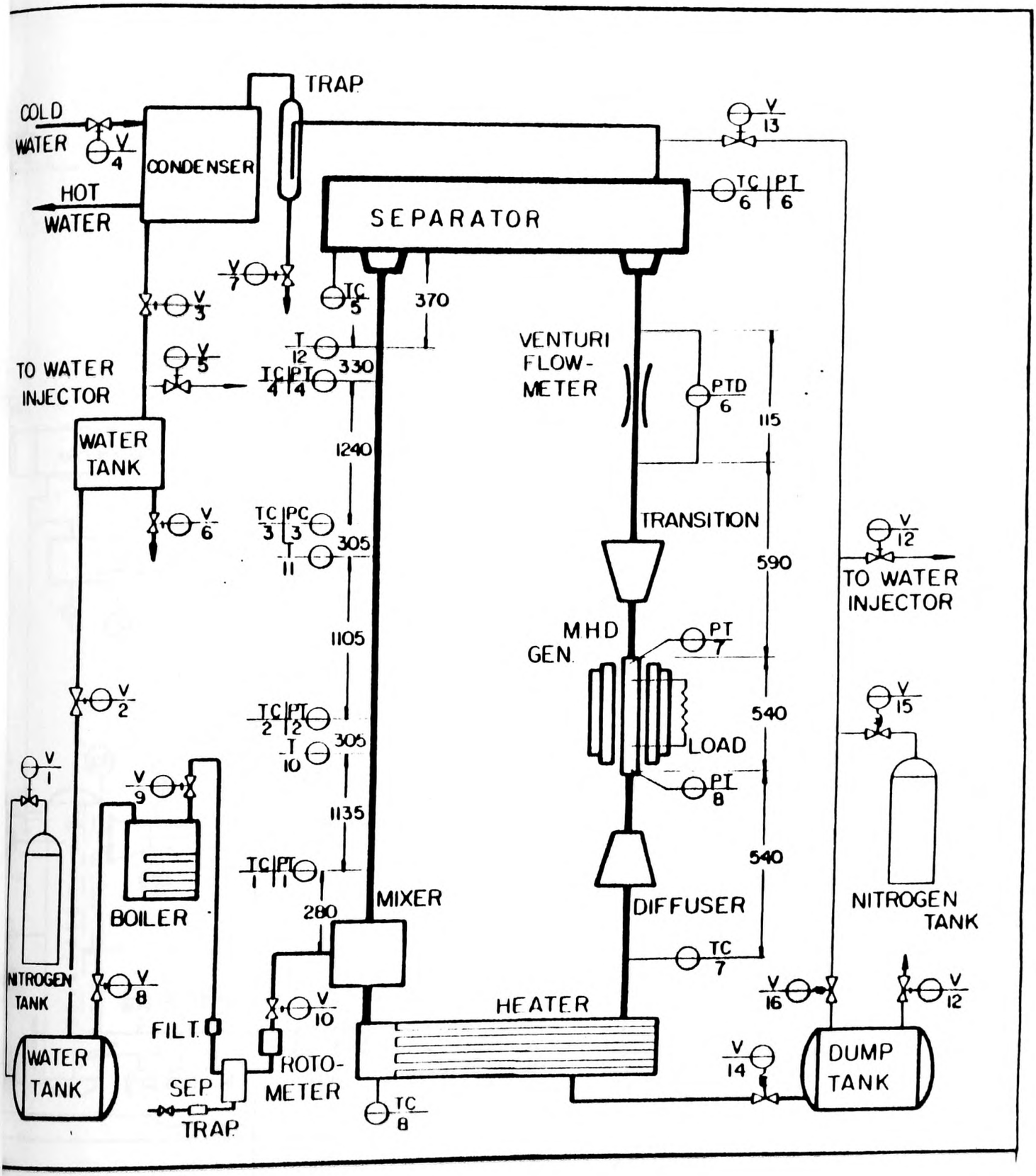

Fig. 3 Schematic of ER-4 experimental facility

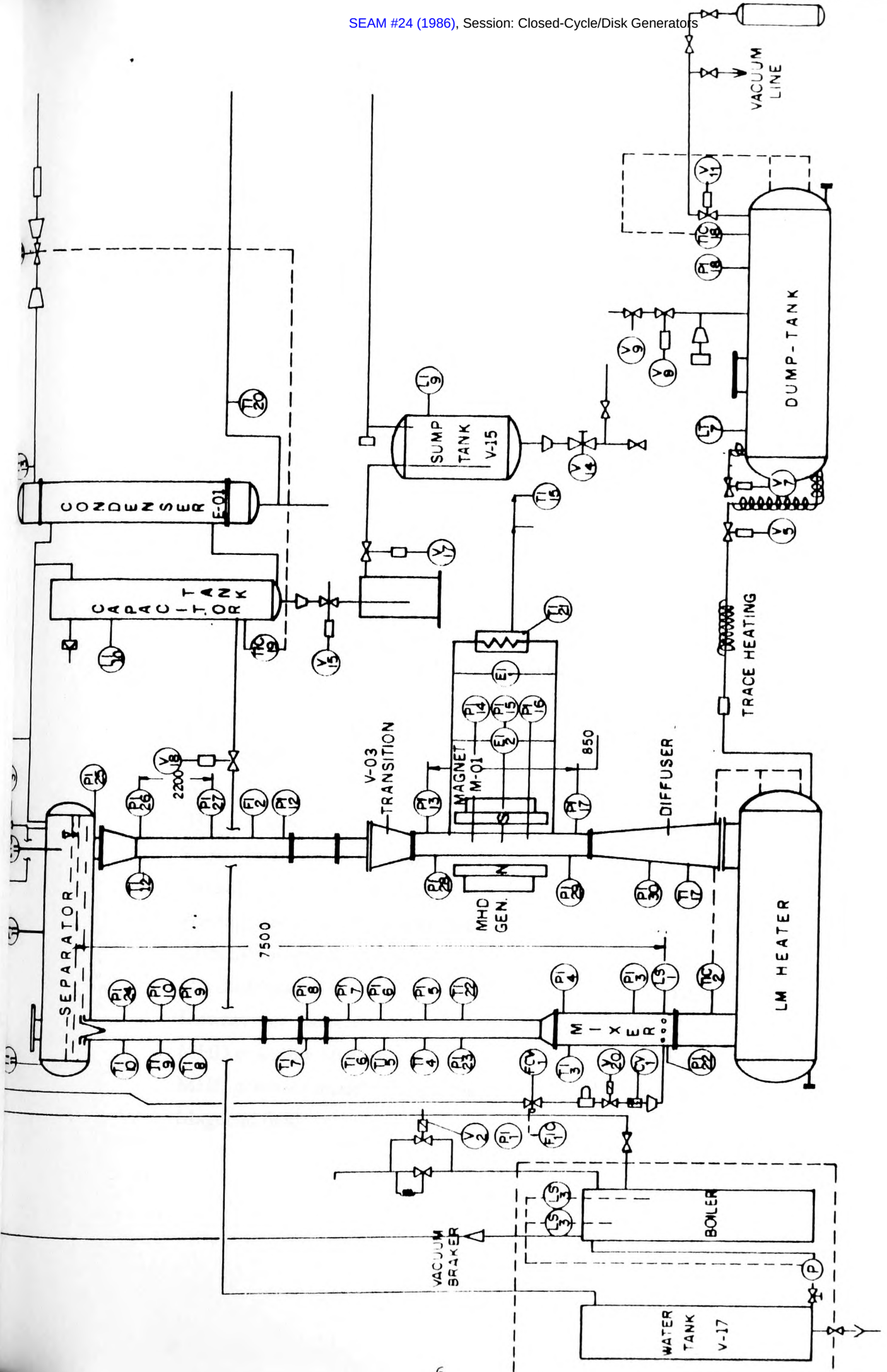

Fig. 4 Schematic of ETGAR-3 experimental facility

* ER-4 system parameters

High temperature in cycle:	431.3 K
Low temperature in cycle	338.6 K
Mixer Pressure	5.34 Bar
Thermal Input	7.0 KW
Liquid metal mass flow rate	65.77 kg/sec
Volatile liquid mass flow rate	0.0026 kg/sec
Average void fraction in upcomer	0.3
Effective height of the system	5.0 m
Upcomer diameter	0.078 m
Downcomer diameter	0.078 m
MHD generator channel width	0.02 m
MHD generation electrode spacing	0.10 m
Magnetic field	0.80 T

* ETGAR-3 system parameters

High temperature in cycle:	423 K
Low temperature in cycle	338 K
Mixer Pressure	4.9 Bar
Thermal Input	97.5 KW
Liquid metal mass flow rate	435.2 kg/sec
Volatile liquid mass flow rate	0.0303 kg/sec
Average void fraction in upcomer	0.4
Effective height of the system	7.5 m
Upcomer diameter	0.203 m
Downcomer diameter	0.203 m
MHD generator channel width	0.06 m
MHD generation electrode spacing	0.15 m
Magnetic field	0.73 T

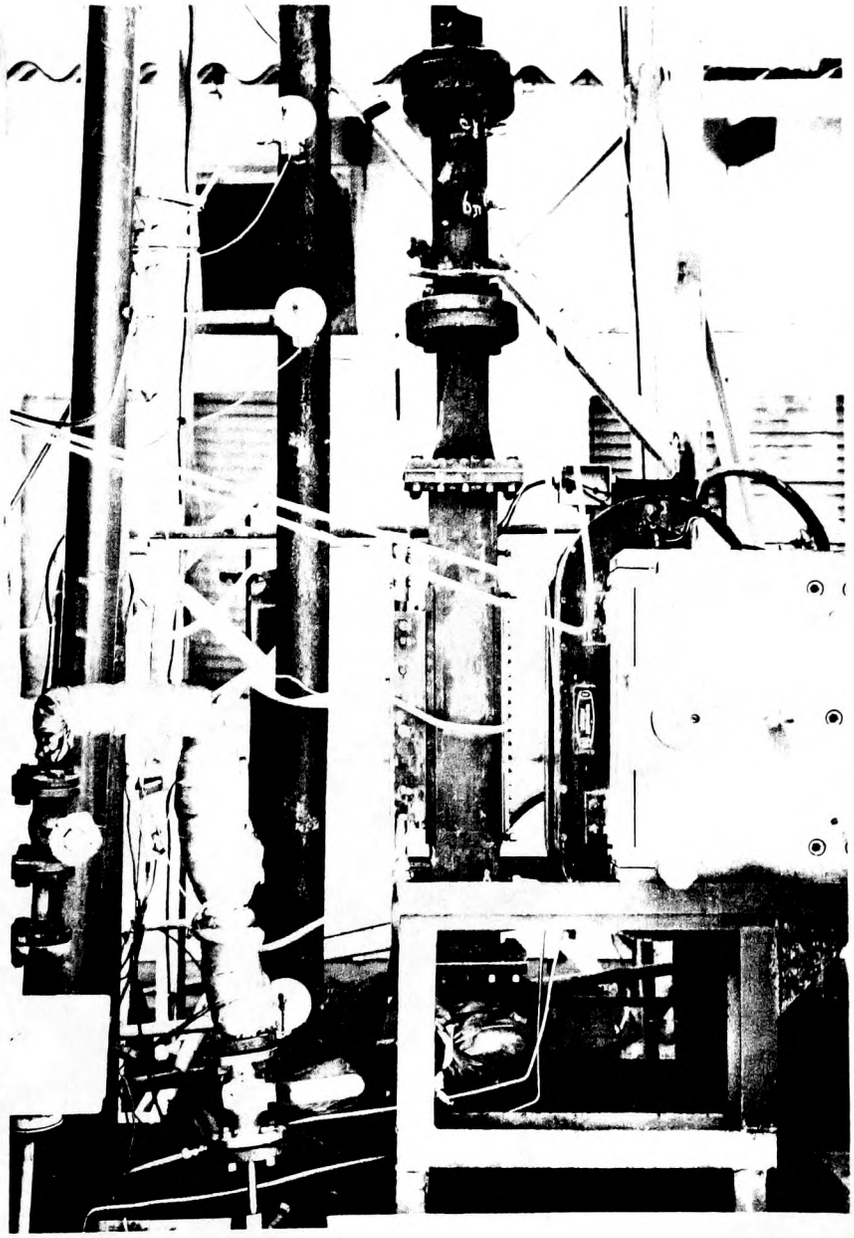

Fig. 5 ER-4 generator assembly

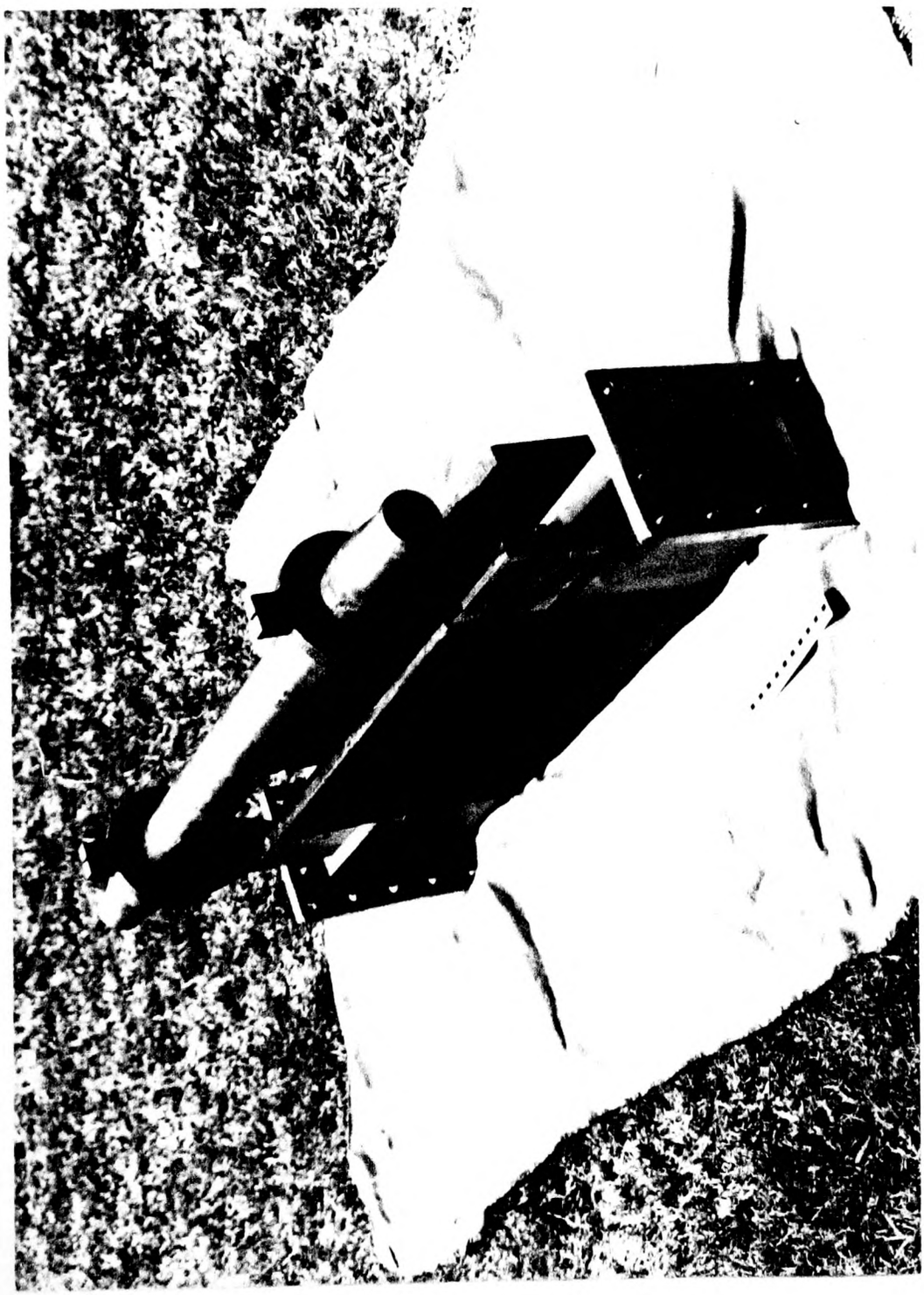

Fig. 6 ETGAR-3 MHD channel assembly

* **Data analysis (for OMACON system)**

• Two phase flow analysis

- Upcomer analysis

Momentum equation:

$$\frac{dp}{dz} = \frac{dp}{dz_{gr}} + \frac{dp}{dz_{acc}} + \frac{dp}{dz_{fr}} \qquad (1)$$

where the gravitational component:

$$\frac{dp}{dz_{gr}} = \left[(1-\alpha)\,\rho_L + \alpha\,\rho_G \right] \cdot g \qquad (2)$$

The accelerational component:

$$\frac{dp}{dz_{acc}} = \left(\frac{m_{TP}}{A}\right)^2 \cdot \frac{d}{dz} \left[\frac{(1-x)^2}{(1-\alpha)\rho_L} + \frac{X^2}{\alpha\,\rho_G} \right] \qquad (3)$$

And the frictional component:

$$\frac{dp}{dz_{fr}} = \phi_{LO}^2 \cdot \left(\frac{dp}{dz}\right)_{fr\ LO} \qquad (4)$$

The Friedel (1979) correlation for the multiplier:

$$\phi_{LO}^2 = E + \frac{3.24 \cdot F \cdot H}{F_r^{0.0454} \cdot W_e^{0.035}} \qquad (5)$$

where:

$$E = (1-X)^2 + X^2 \cdot (\rho_L/\rho_G) \cdot (f_{GO}/f_{LO}) \quad (6)$$

$$F = X^{0.78} \cdot (1-X)^{0.224} \quad (7)$$

$$H = (\rho_L/\rho_G)^{0.91} \cdot (\mu_G/\mu_L)^{0.19} \cdot (1-\mu_G/\mu_L)^{0.7} \quad (8)$$

$$F_r = (m_{TP}/A)^2 / (g \cdot D \cdot \rho^2_{TP}) \quad (9)$$

$$W_e = (m_{TP}/A)^2 \cdot D/(\rho_{TP} \cdot \sigma) \quad (10)$$

The two-phase density:

$$\rho_{TP} = [(1-X)/\rho_L + X/\rho_G)]^{-1} \quad (11)$$

The mixture quality:

$$X = m_G/(m_G + m_L) \quad (12)$$

and the gas void fraction

$$\alpha = \rho_L \cdot X / (\rho_L \cdot X + S \cdot (1-X) \rho_G) \quad (13)$$

In case of non-complete separation (carry-under phenomena):

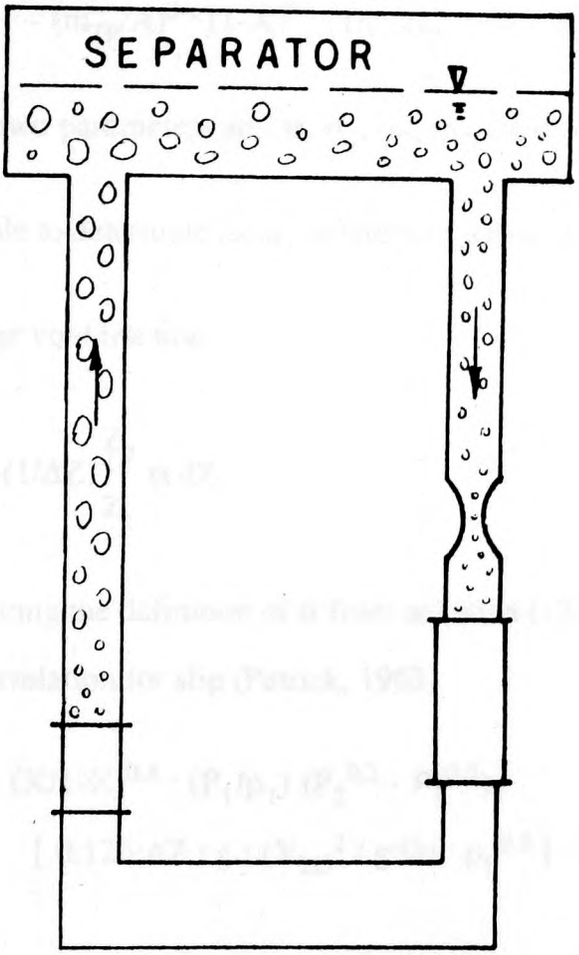

The void fraction at the downcomer is to be evaluated.

- Downcomer carry-under analysis

Momentum equation

$$\frac{dp}{dz} = \frac{dp}{dz_{gr}} - \frac{dp}{dz_{acc}} - \frac{dp}{dz_{fr}} \qquad (14)$$

where the three right terms are similar to the upcomer.

By integration of equation (14) between two points:

$$P_2 - P_1 = [(1-\alpha)\rho_L + \alpha\rho_G] \cdot g \cdot \Delta Z - \phi_{LO}^2 \cdot \Delta P_{frLO} - \\ - (m_{TP}/A)^2 \cdot (1-X)^2 \cdot [1/(1-\alpha_2) - 1/(1-\alpha_1)] / \rho_L \qquad (15)$$

The unknown parameters are: α, α_1, α_2, m_{TP} and ϕ_{LO}^2.

It is possible to determine these variables in terms of x:

The average void fraction:

$$\alpha = (1/\Delta Z) \int_{Z_1}^{Z_2} \alpha \, dZ \qquad (16)$$

by substituting the definition of α from equation (13)

and the correlation for slip (Petrick, 1963).

$$\alpha = (X/1-X)^{0.8} \cdot (P_1/\rho_1) (P_2^{0.2} - P_1^{0.2}) / \\ [\, 0.126 \cdot \Delta Z \cdot g \cdot (V_{LO}^2 / g \cdot D) \cdot \rho_L^{0.2} \,] \qquad (17)$$

$$\alpha_1 = 1 / [\, 1 + (1-X) \cdot S \cdot \rho_{G1} / X \cdot \rho_L \qquad (18)$$

$$\alpha_2 = 1 / [\, 1 + (1-X) \cdot S \cdot \rho_{G2} / X \cdot \rho_L \qquad (19)$$

The mixture mass flow rate, m_{TP}, measured by venturi flow meter

and corrected to two-phase flow by an equivalent density ρ_E

is suggested by Kinghorm (1985) to be:

$$1/\rho_E = [\, X/\rho_G + S \cdot (1-X) / \rho_L] \cdot [\, X + (1-X) / S \,] \qquad (20)$$

The multiplier ϕ_{LO}^2 similar to the upcomer correlated by Friedel (1979):

$$\phi_{LO}^2 = F(X) \tag{21}$$

Equations (15), (17), (18), (19), (20) and (21) are solved by an interative process.

The output gives the gas mass flow rate at the downcomer:

$$m_{GD} = X_D \cdot m_L \tag{22}$$

The downcomer gas mass flow rate has to be added to the boiler gas mass flow rate injected through the mixer:

$$m_{GT} = m_{G1} + m_{GD} \tag{23}$$

The new mixture quality in the upcomer is:

$$X = m_{GT} / (m_{GT} + m_L) \tag{24}$$

For the upcomer, one-dimensional dynamical equation is solved by a computer code, IDent. The output of this code is the void fraction as a function of the position along the upcomer by inputs of measured pressure along the upcomer.

- System Performance Analysis:

  - Total generator efficiency

$$\eta_{GEN,TOT} = W_e / (\dot{Q} \cdot \Delta P_{GEN}) \qquad (25)$$

  - Electrical generator efficiency (excluding friction losses)

$$\eta_{GEN,e} = W_e / [\dot{Q}_{LM} \cdot (\Delta P_{GEN} - \Delta P_{frGEN})] \qquad (26)$$

  - Theoretical generator efficiency, calculations based on Sutton (1962)

  - Experimental cycle efficiency

$$\eta_{EXP} = W_e / \text{HEAT INPUT} \qquad (27)$$

  - Theoretical cycle efficiency calculated by computer code "ETGAR 3"

* **Experimental Results:**

• ER-4 System

- Void fraction distribution along the upcomer. In Fig. 7 it is seen that the void fraction increases with the height, and also that the local void fraction increases with increasing of gas mass flow rate, at the same superficial liquid velocity.

- Average void fraction as function of quality at three different elevations. From Fig. 8 it can be seen that the average void fraction increases when the quality and height increases.

- Comparison of experimental slip ratio with modified Smissaert slip correlation. In Figs. 9,10 it can be seen that the local slip ratio increases with the height, and decreases with superficial liquid velocity increase, the slip ratio increases rapidly in the upper plennum of the riser.

Modified Smissaert correlation based on the following assumption:

$S \leq 1 \qquad S_m = 1$

$S > 1 \qquad S_m = S_{Smiss.}$

In the above figures all the local experimental slip values are greater than the Smissaert correlation values.

- Comparison of average experimental slip ratio with correlations of Baroczy (1965) and Smissaert (1963) in the middle section of the upcomer vs. quality. In Fig. 11 it can be seen clearly that the Baroczy correlation is totally incompatible while the Smissaert correlation shows better agreement with experimental values.

- Deviation density of experimental slip to Smissaert modified slip correlation. From Fig 12 it seems that the typical deviation of the Smissaert correlation from experimental values is about 10%.

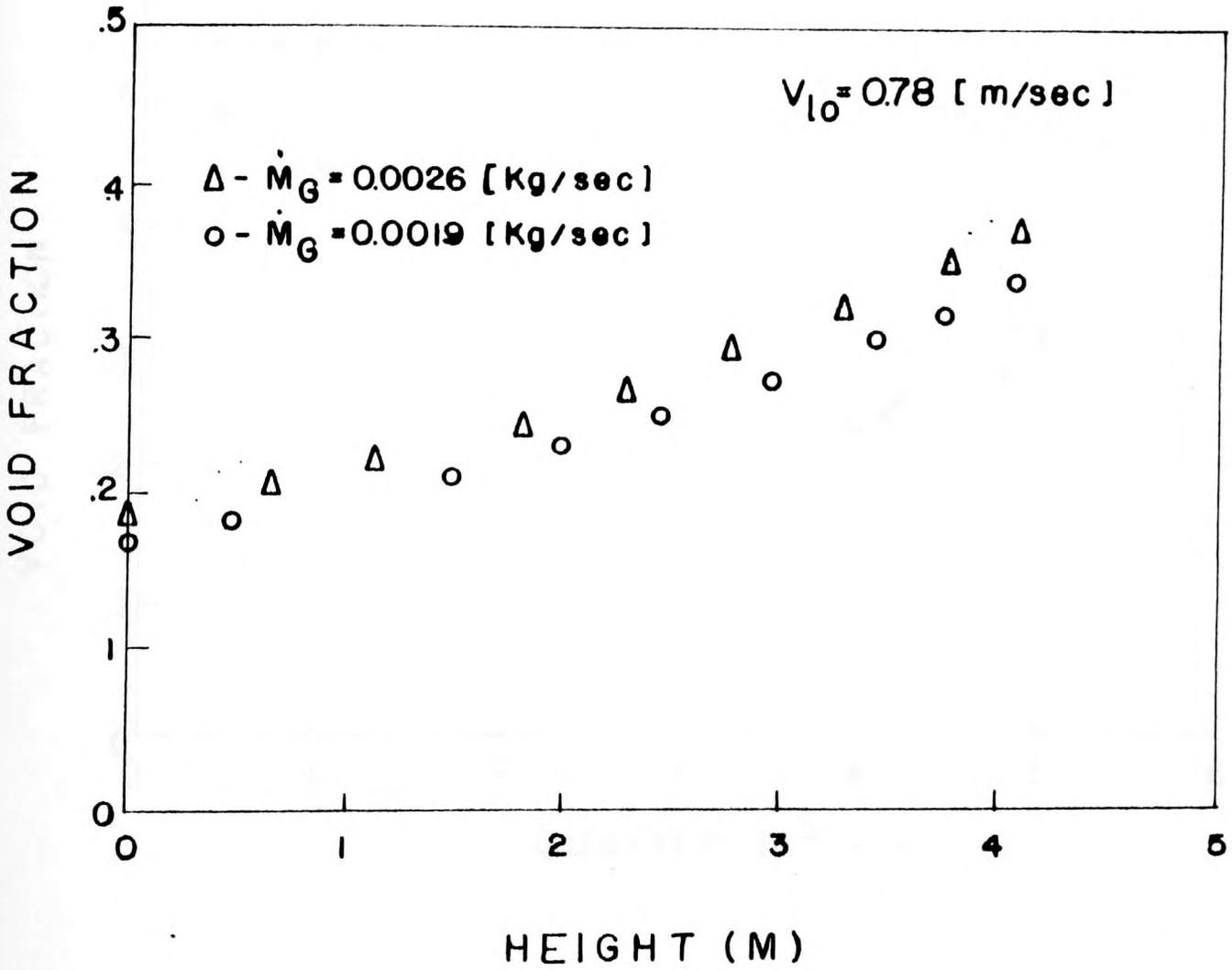

Fig. 7 Void fraction distribution along the upcomer

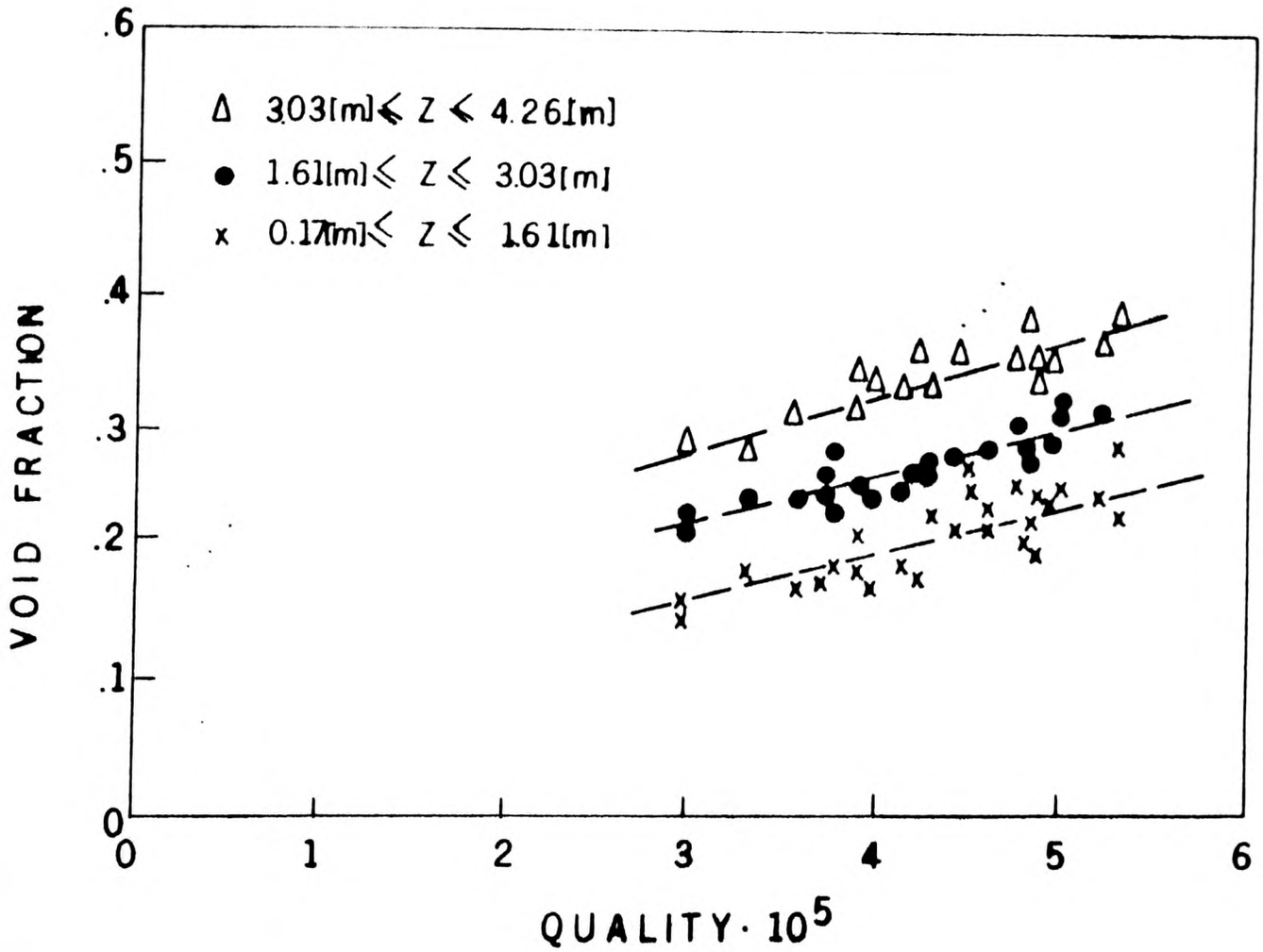

Fig. 8 Average void fraction as a function of quality at three different elevations

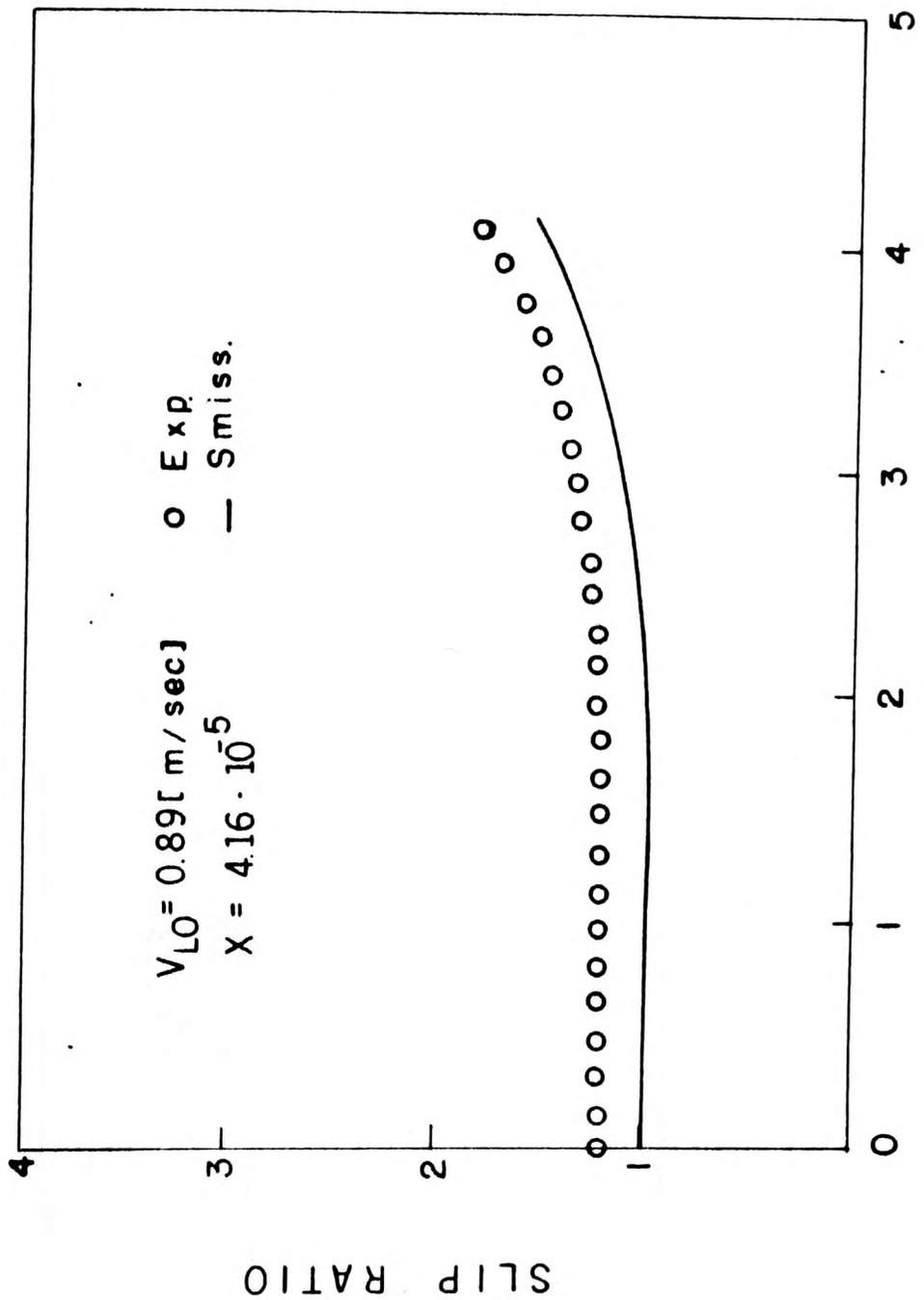

Fig. 9 Comparison of experimental slip ratio with modified Smissaert slip correlation (superficial velocity - 0.89 m/sec)

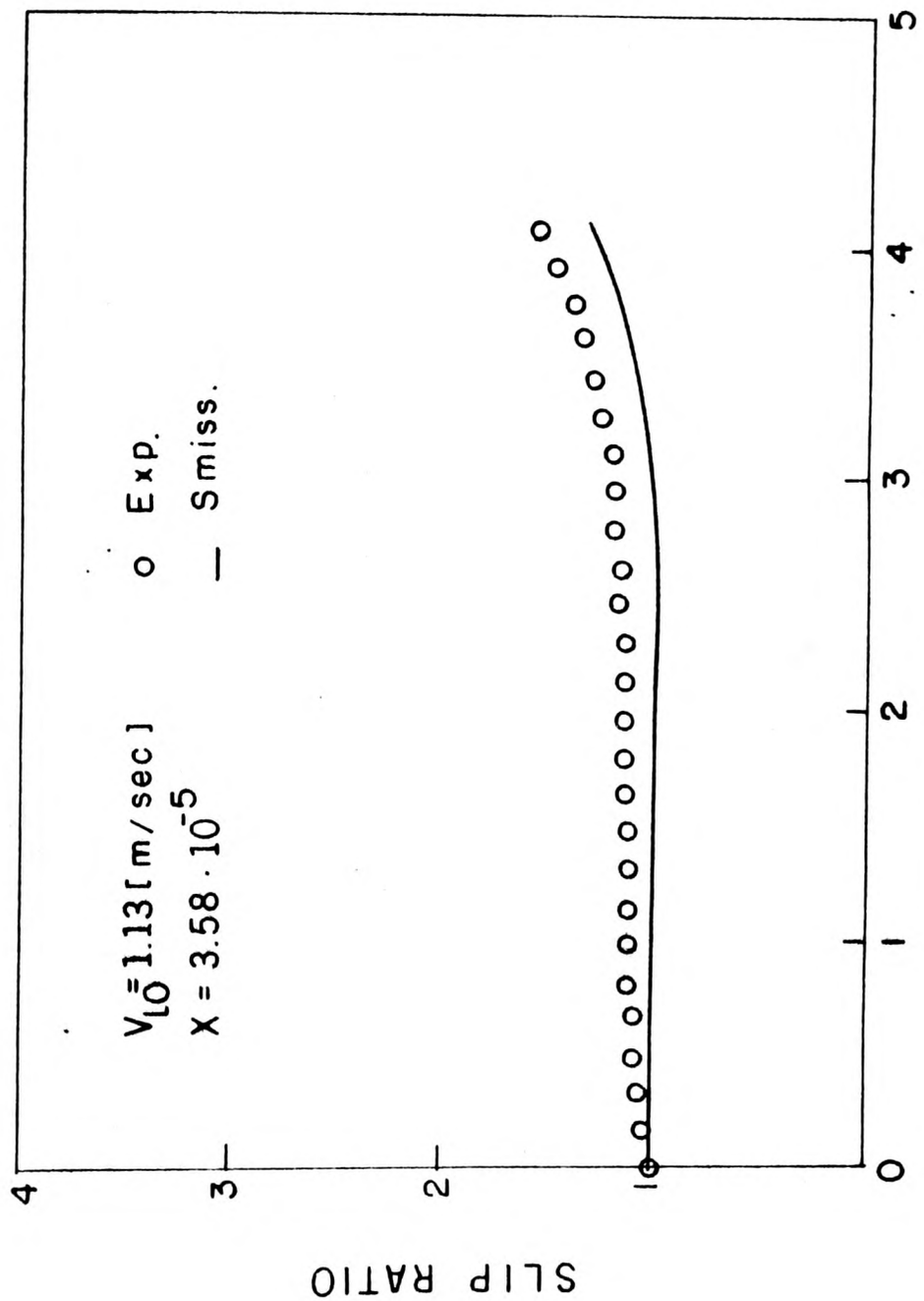

Fig. 10 Comparison of experimental slip ratio with modified Smissaert slip correlation (superficial velocity - 1.13 m/sec)

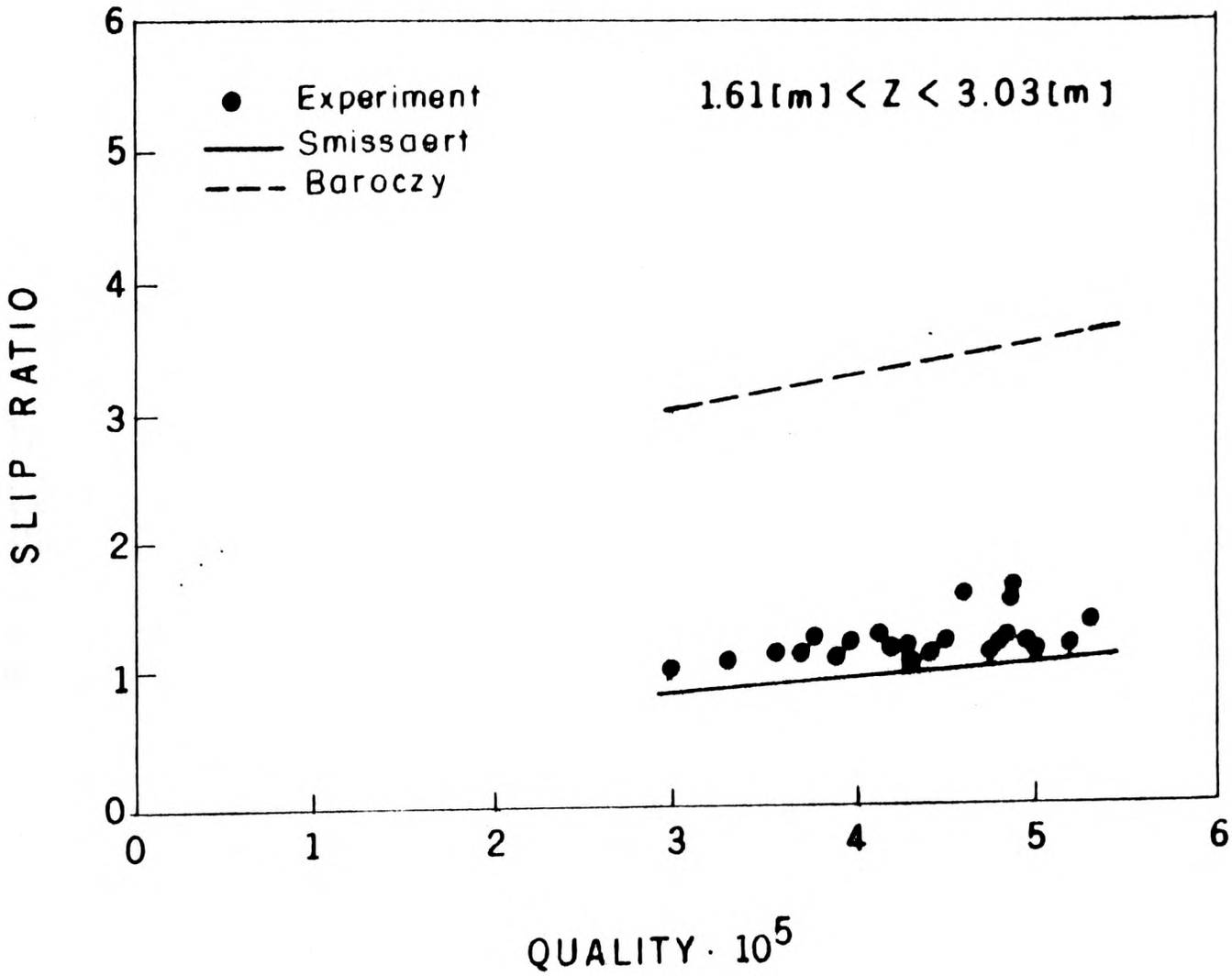

Fig. 11 Comparison of experimental average slip ratio with slip correlations vs. quality

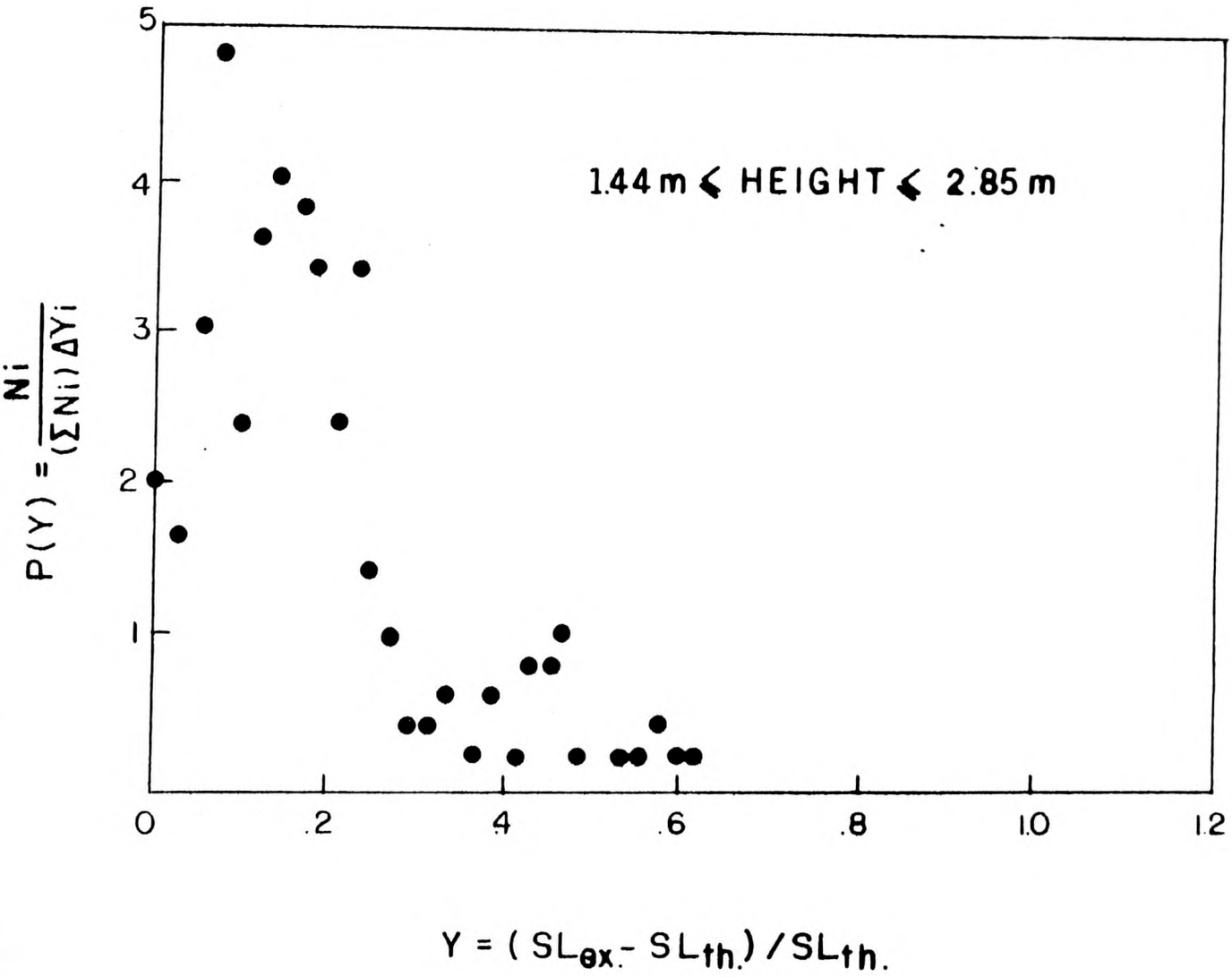

Fig. 12 Deviation density of experimental slip to modified Smissaert slip correlation

- Electrical power output vs. gas flow rate with different magnetic fields. As can be seen in Fig. 13 the electrical power output increases with the gas flow rate and the magnetic field, up to an optimal value. It can be explained that by increasing magnetic field, the friction losses decrease; on the other hand, the slip ratio increases due to the superficial liquid velocity reduction.

- Total generator efficiency vs. liquid volumetric flow rate. The generator total efficiency shown in Fig. 14 decreases with liquid volumetric flow rate due to the increase of friction losses.

- Electrical generator efficiency vs. liquid metal volumetric flow rate. The electrical generator efficiency, excluding friction losses, is not affected by liquid volumetric flow rate, as shown, and one observes good agreement with theoretical generator efficiency calculated according to Sutton (1962), as shown in Fig. 15.

- Experimental cycle efficiency vs. theoretical cycle efficiency. From Fig. 16 it can be seen that the agreement between experimental and theoretical cycle efficiency improved at higher cycle efficiencies.

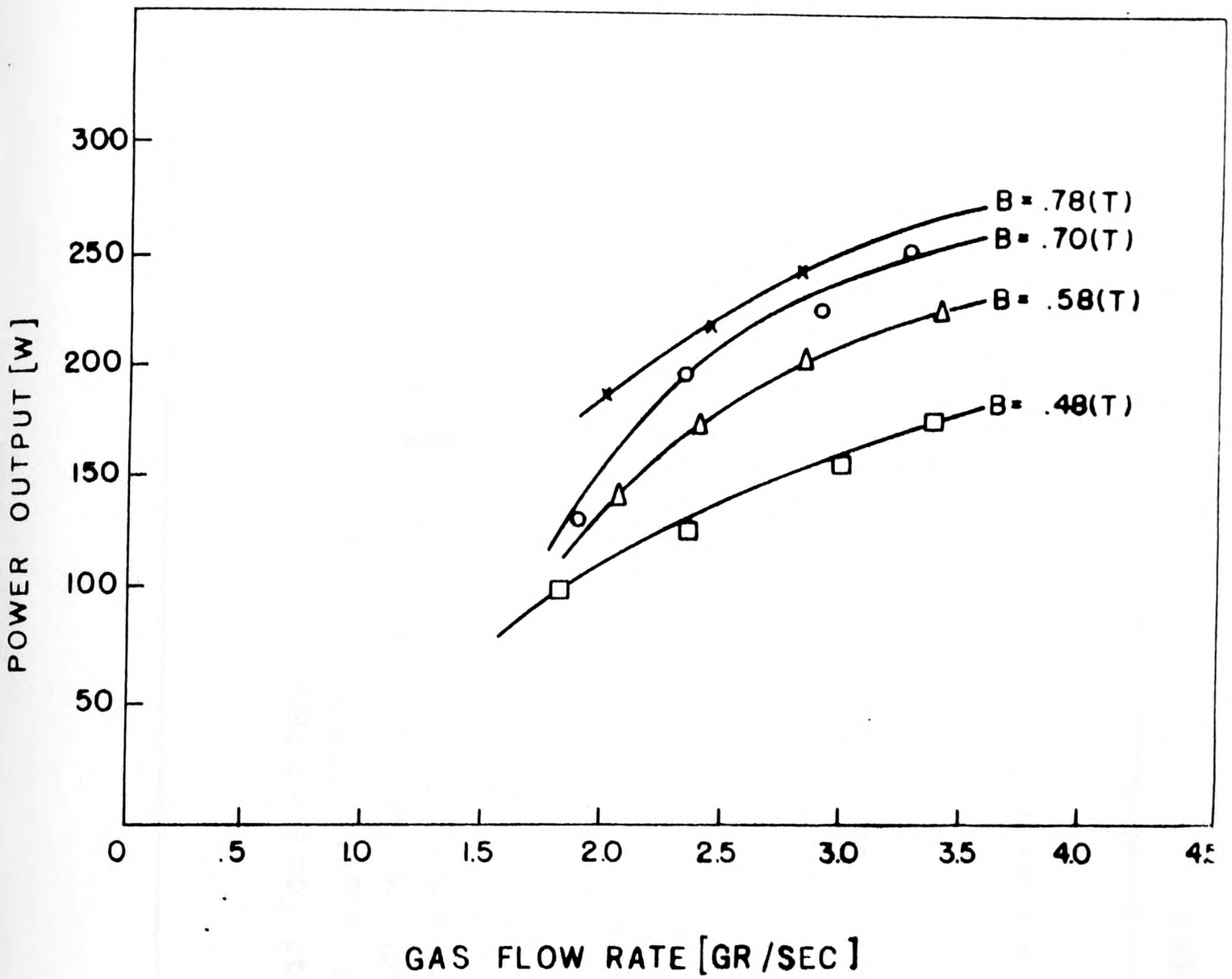

Fig. 13 Electrical power output vs. gas flow rate at different magnetic fields (ER-4)

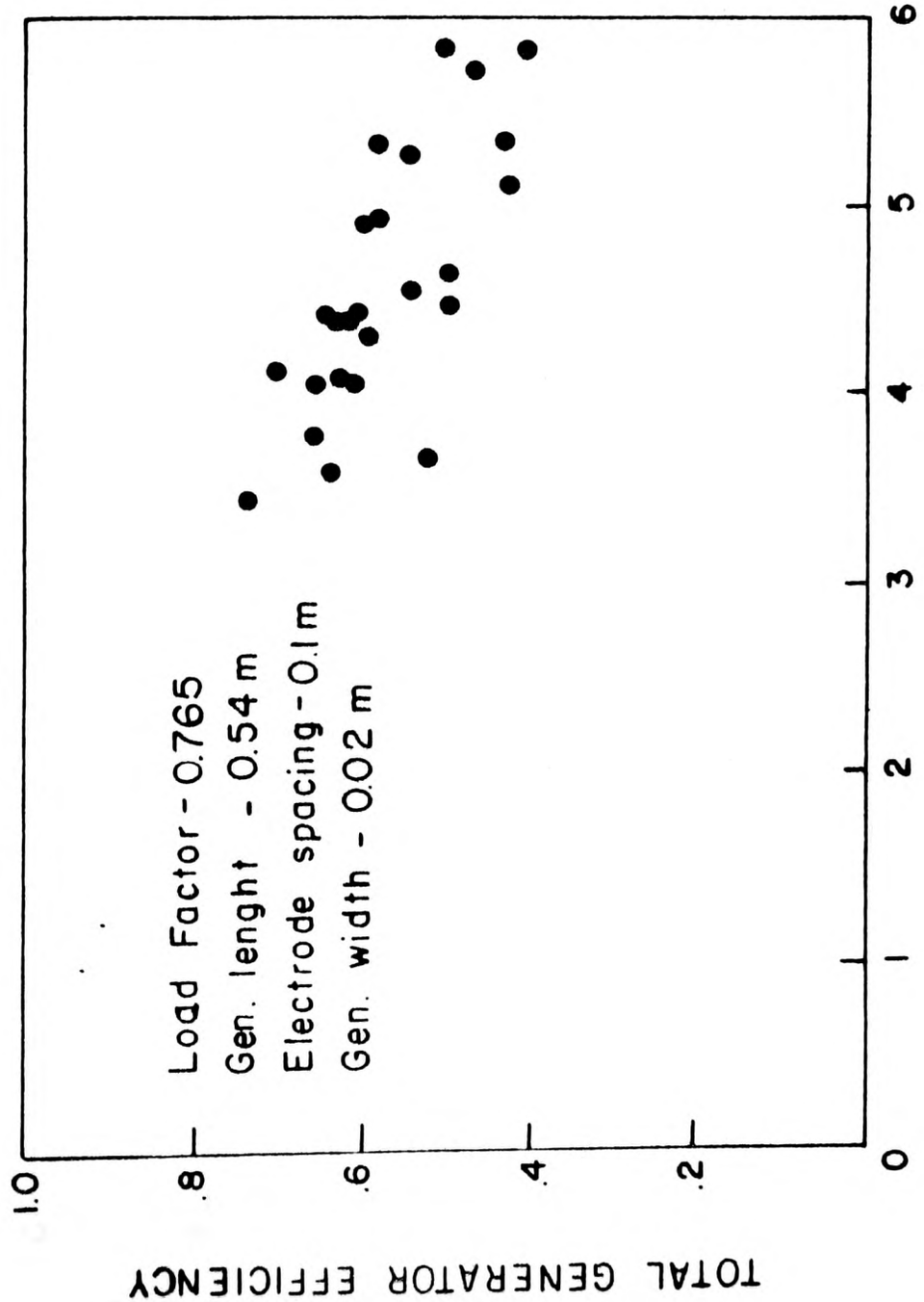

Fig .14 Total generator efficiency vs. liquid metal volumetric flow rate

(ER-4)

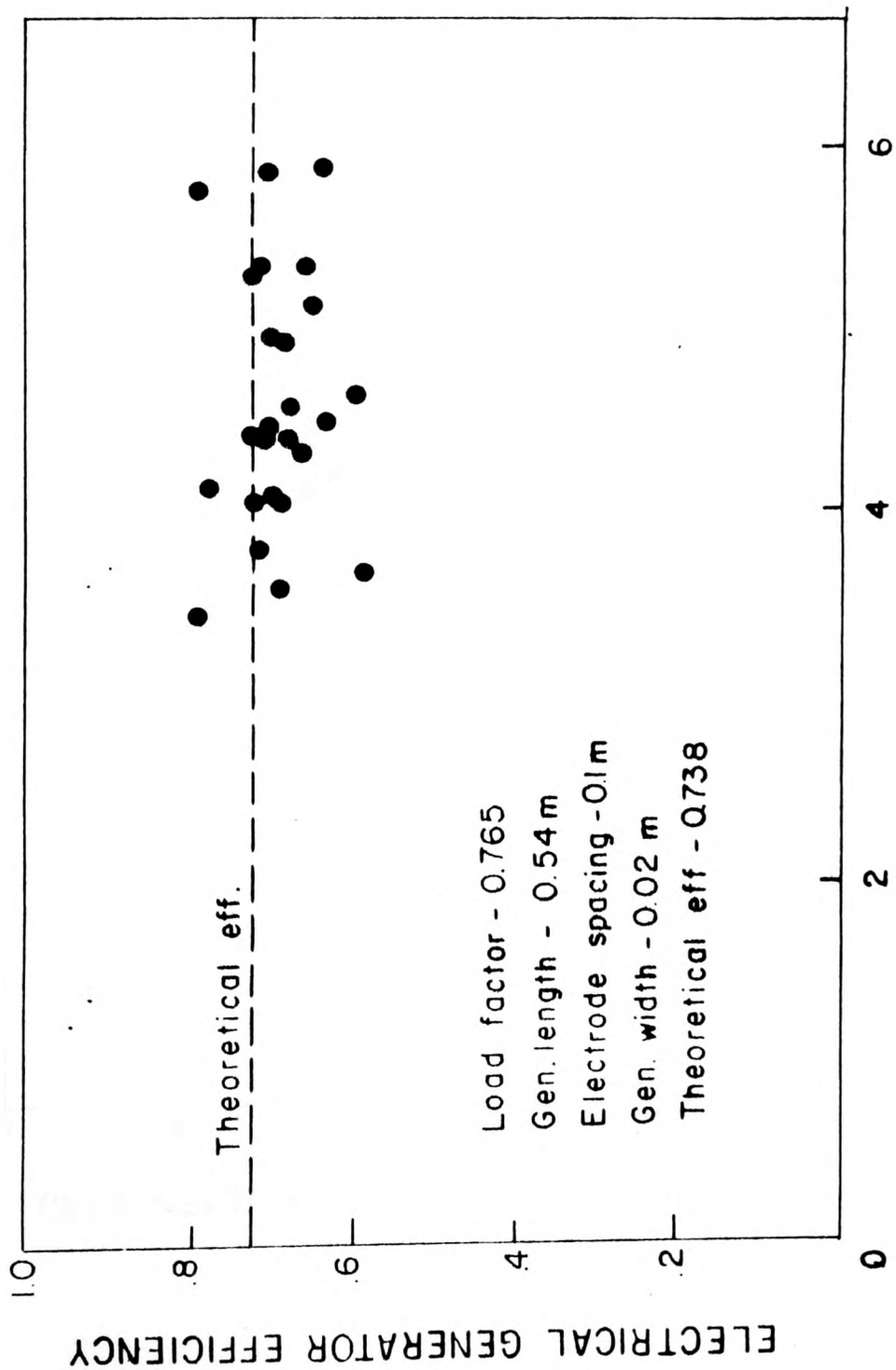

Fig. 15 Electrical generator efficiency vs. liquid metal volumetric flow rate

(ER-4)

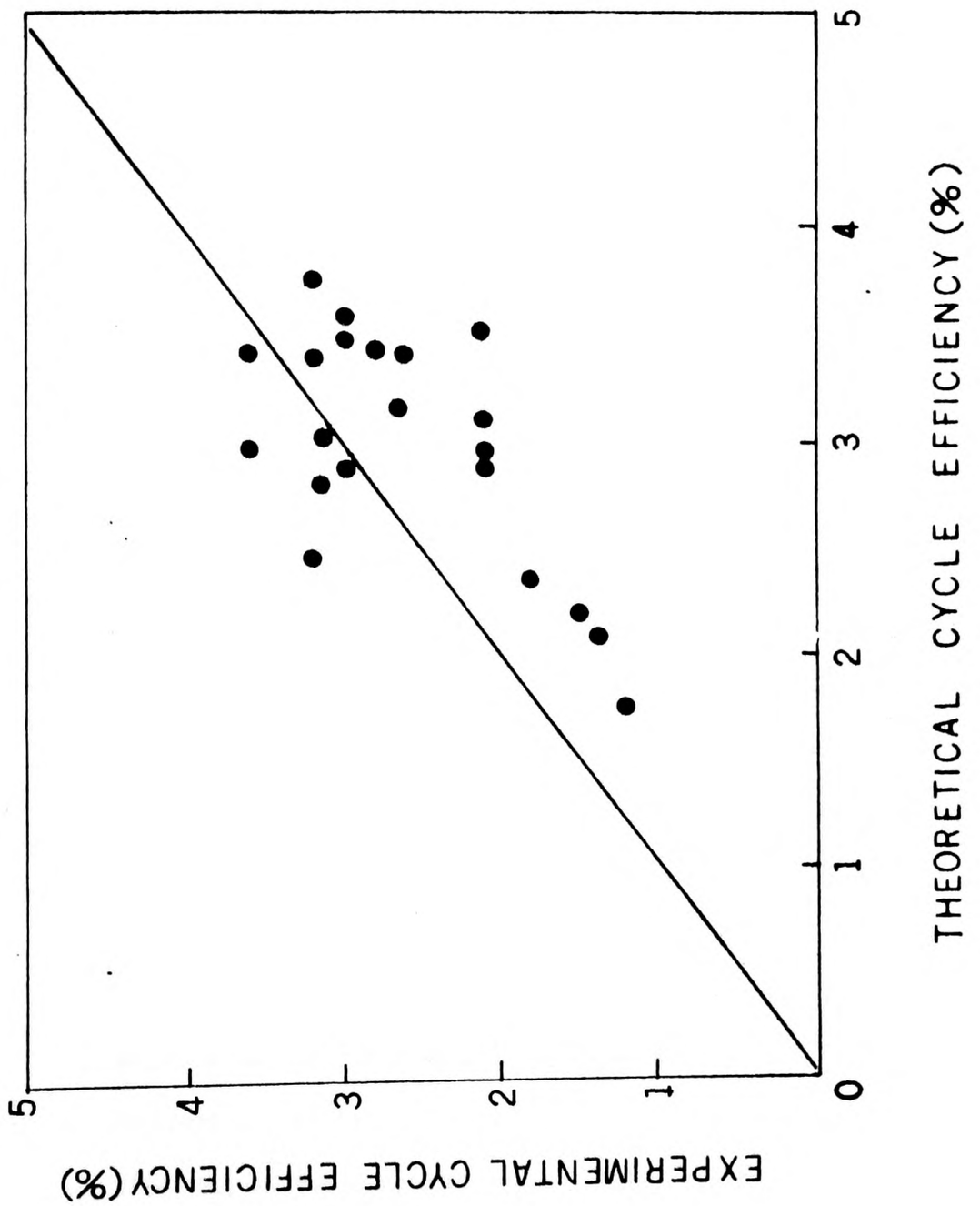

Fig. 16 Experimental cycle efficiency vs. theoretical cycle efficiency (ER-4)

- ETGAR-3 System
  - Total generator efficiency vs. liquid metal velocity in generator.

    The generator total efficiency shown in Fig. 17 decreases with the liquid metal velocity due to the increase of friction losses.
  - Electrical generator efficiency vs. liquid metal velocity in the generator.

    The electrical generator efficiency excluding friction losses as shown in Fig. 18 is not affected by the liquid metal velocity in the generator.

    A good agreement can be observed with the theoretical generator efficiency.
  - Generator voltage output vs. liquid metal velocity in generator.

    In Fig. 19 a linear increase of voltage with the magnetic field and with liquid metal velocity in the generator for different magnetic fields.

    All curves direct towards the origin.
  - Electrical power output vs. gas flow rate with different magnetic fields.

    As can be seen in Fig. 20 the electrical power output increases with increase of steam flow rate, and with the magnetic field until an optimal value. It is seen that the power output reaches an asymptotic value at high steam flow rates.
  - Experimental cycle efficiency vs. steam flow rate.

    Fig. 21 illustrates a high dependency of the cycle efficiency on the steam flow rate. The efficiency decreases with the steam flow rate increase due to the increase of the slip ratio. The experimental cycle efficiency increases with the magnetic field up to optimal value.
  - Experimental cycle efficiency vs. theoretical cycle efficiency. From Fig. 22 one can see that most of the experimental efficiency points are lower than the theoretical points due to higher values of experimental slips in the riser than those which were calculated, using modified Smissaert correlation.

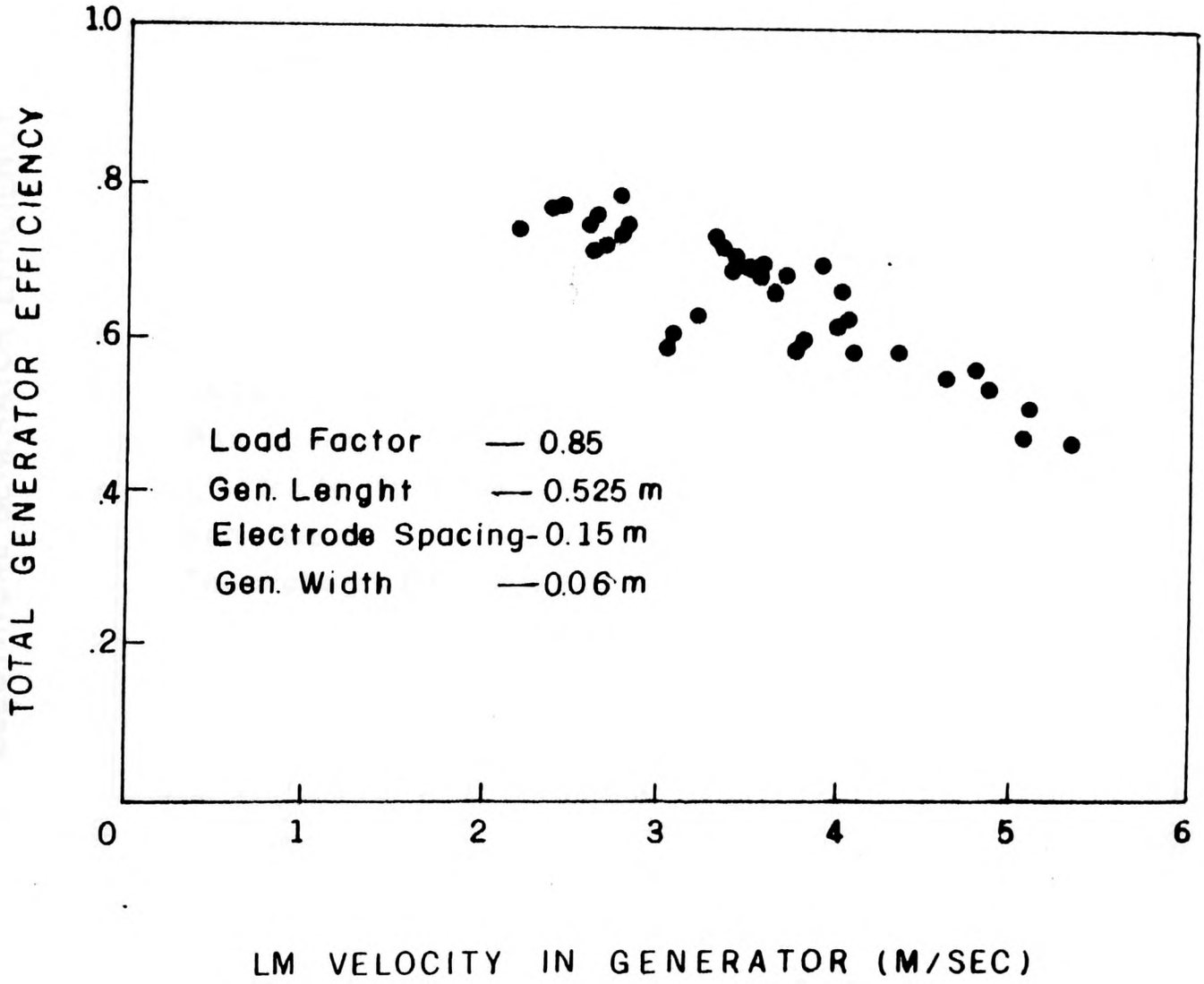

Fig. 17 Total generator efficiency vs. liquid metal velocity in generator (ETGAR-3)

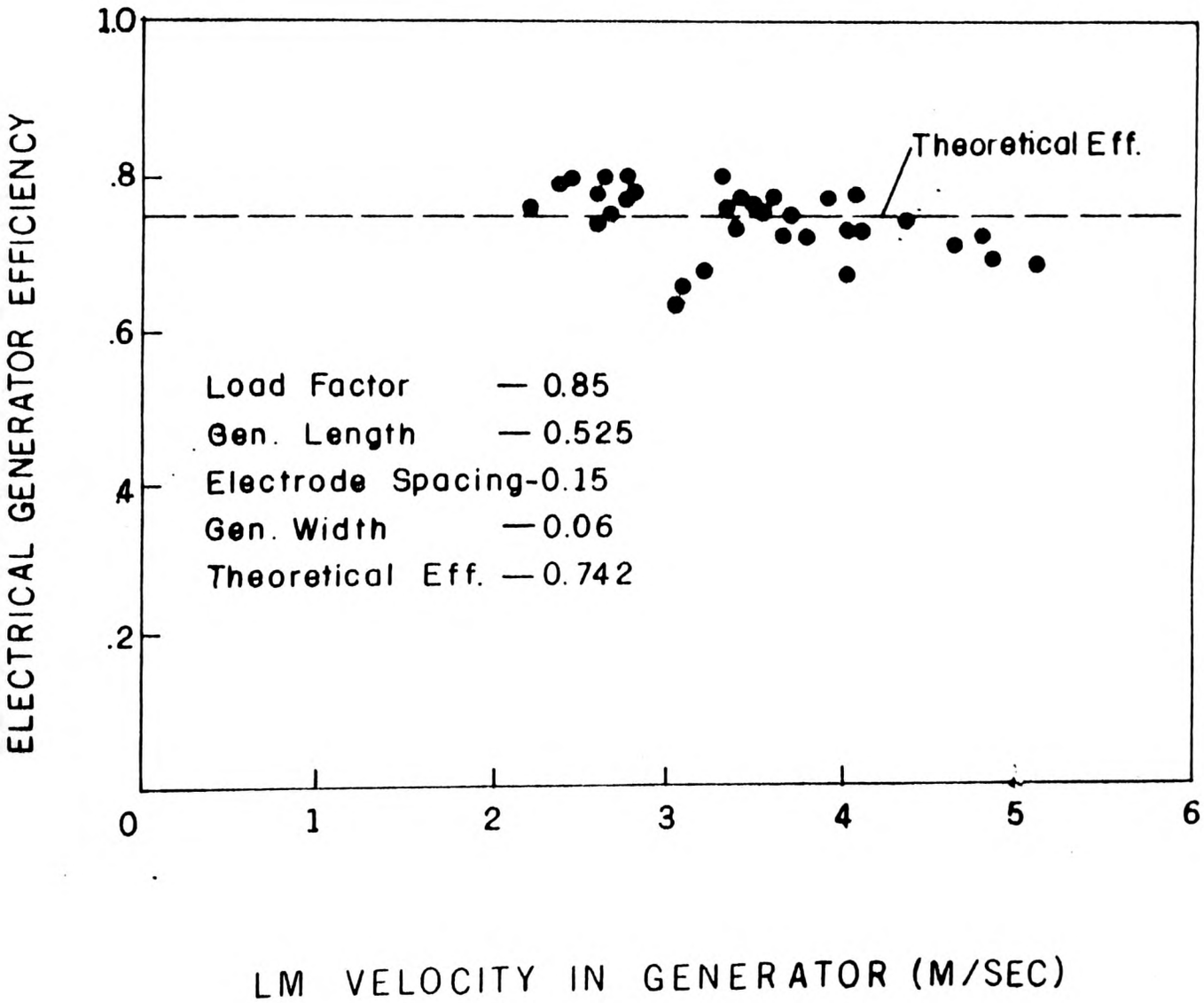

Fig. 18 Electrical generator efficiency vs. liquid metal velocity in generator (ETGAR-3)

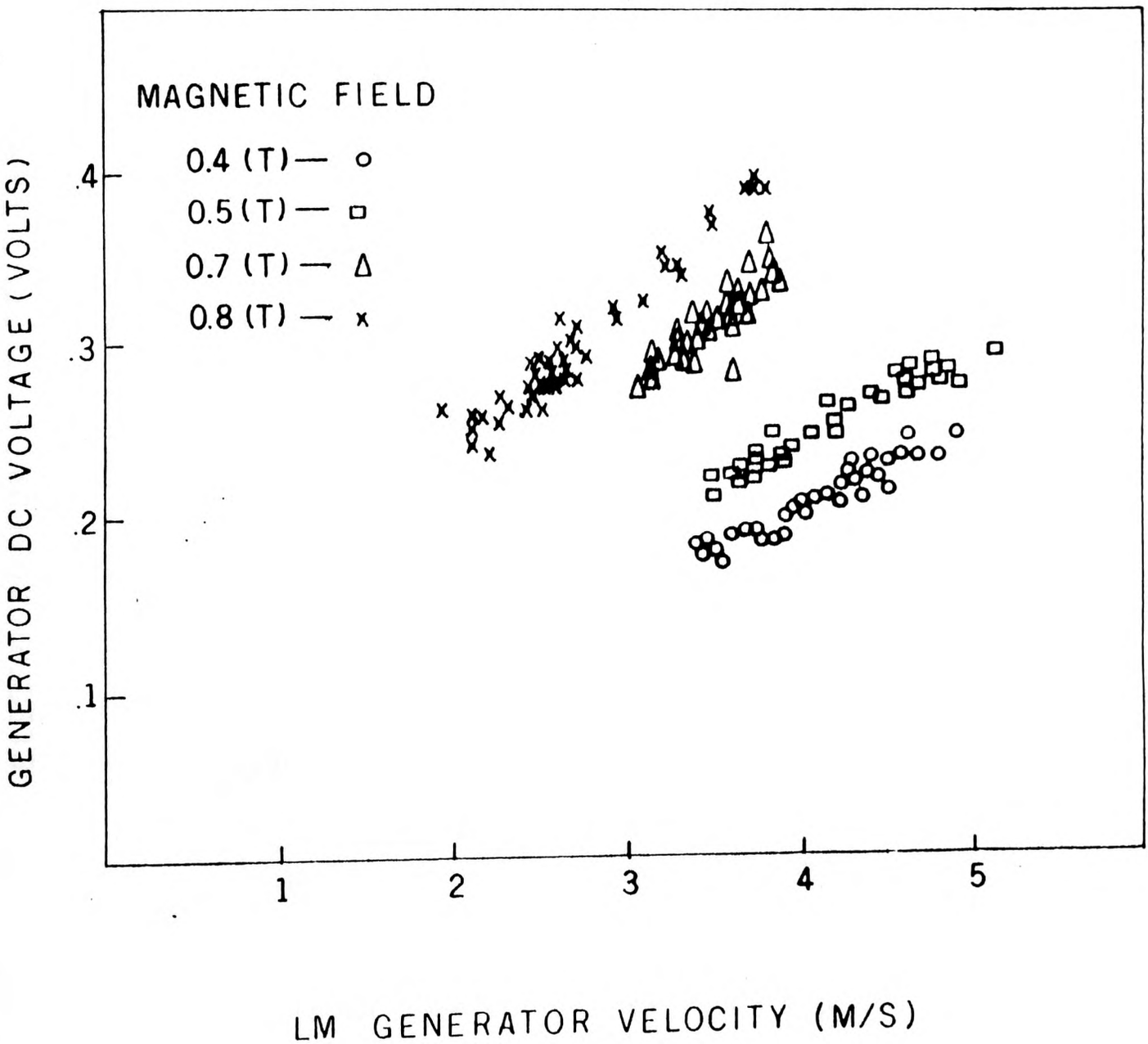

Fig. 19 Generator DC voltage vs. liquid metal velocity in generator with different magnetic fields (ETGAR-3)

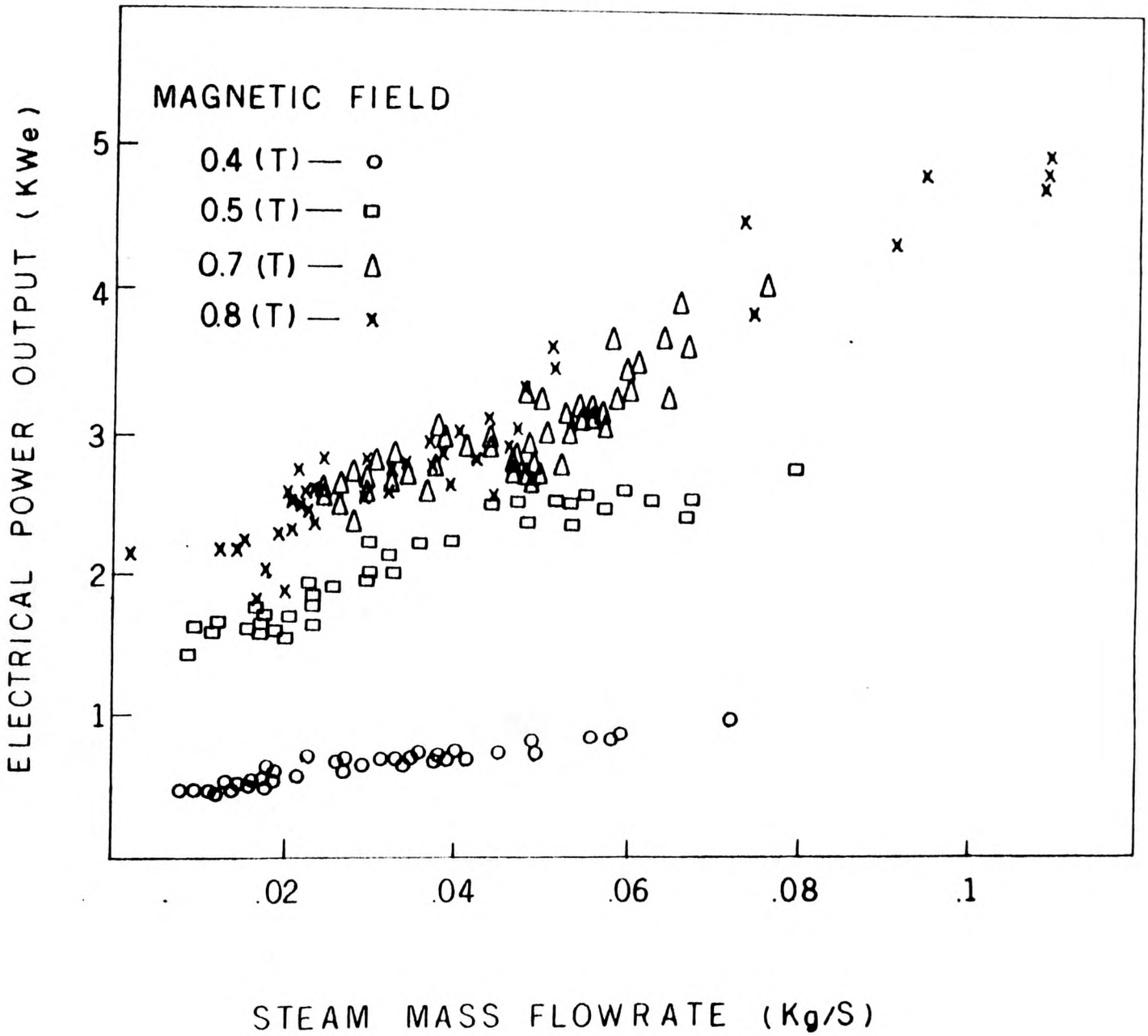

Fig. 20 Electrical power ouput vs. steam mass flow rate with different magnetic fields (ETGAR-3)

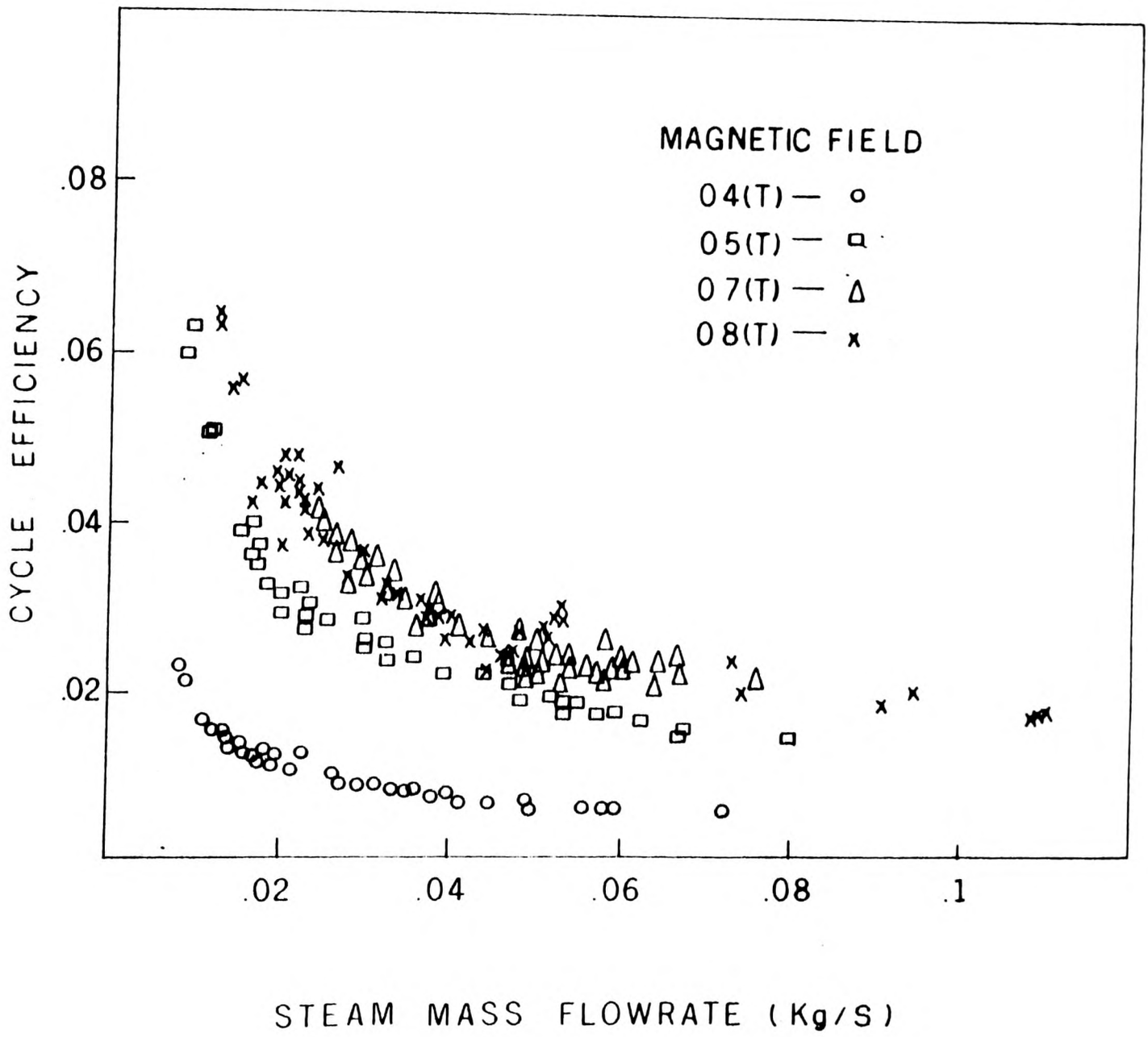

Fig. 21 Cycle efficiency vs. steam mass flow rate with different magnetic fields (ETGAR-3)

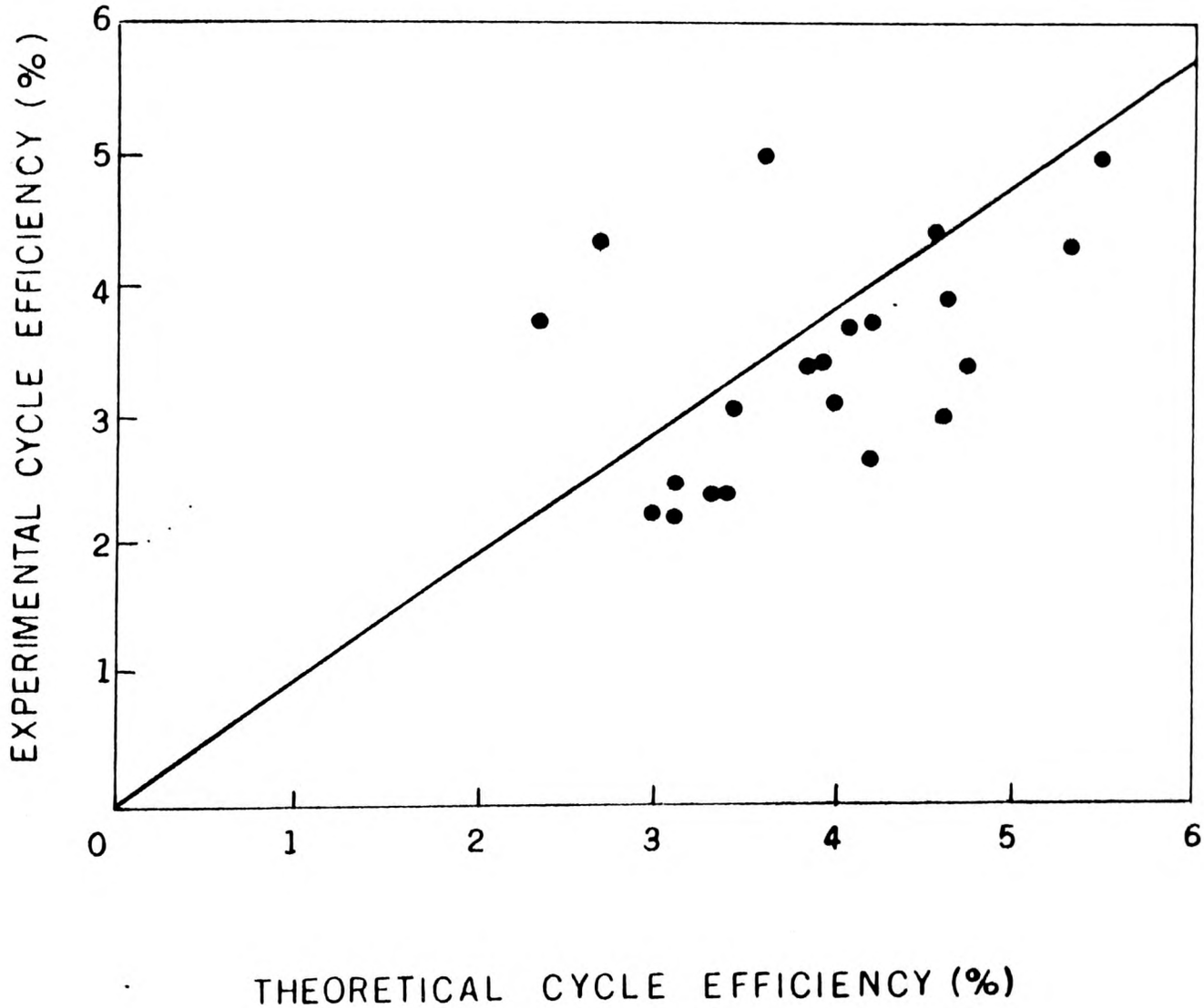

Fig. 22 Experimental cycle efficiencies vs. theoretical cycle efficiencies (ETGAR-3)

* CONCLUSIONS

The experimental results presented and analyzed above and their comparison with empirical correlations suggested by a number of authors lead to the following conclusions:

a) All the presently available data on void fraction and slip values in upwards two-phase heavy liquid metals flows in the flow quality range $2.98.10^{-5} \leq x \leq 5.32.10.^{-5}$ for ER-4 and $2.5 \times 10^{-5} \leq 3 \times 10^{-4}$ for Etgar-3, and superficial velocity range 0.793 (m/s) $\leq V_{LO} \leq$ 1.219 (m/sec) for ER-4 and 0.6 - 1.5 m/sec for Etgar-3 are best approximated by the Smissaert correlation providing that the latter is modified so that it would not give slip values less than unity ($S = S_{Smiss}$ at $S_{Smiss} \geq 1$ and $S = 1$ at $S_{Smiss} < 1$).

b) Experimental slip values are usually higher than values calculated according to Smissaert's correlation (modified as above), the deviation being higher for the inlet section (adjacent to mixer) and outlet section (adjacent to separator tank) of the pipe and lower, but still substantial, for the middle section where the flow was presumably stabilized. It has to be kept in mind that Smissaert's correlation was derived from experimental data at much lower superficial velocity values [$V_{LO} \leq$ 0.330 (m/sec)] and also that these experimental data have been obtained under conditions when special measures have been taken to secure wetting of the walls of the pipe by mercury, while in the present study no such measures have been taken.

c) Comparison of the actual performance of the energy conversion system (electrical power output, overall conversion efficiency with calculations based on modified Smissaert's correlation for slip and Friedel's correlation for friction losses in two-phase flow showed a fair coincidence, while the experimental values of efficiency are lower than calculated at extreme off-design working conditions and tend to become equal to calculated values (with ± 15% scatter) when working conditions are approaching the design point.

d) Comparison of the generator electrical efficiency (excluding friction losses) of Etgar-3 and ER-4 facilities shows good agreement with theory. One can use this theory (machinery) for the design of single phase MHD generators with confidence.

e) In assessment of results described above, it should be kept in mind that in all of the experiments there was a carry-under of steam into the downcomer. The influence of this phenomena on the results was cancelled out through the relevant calculation procedure described in this report. However, it is highly desirable to arrange additional experiments with a different design of separator which would eliminate the carry-under phenomena. Only after this is done can final conclusions be made regarding the appropriate methods of predicting characteristics of two-phase flows in vertical pipes.

* REFERENCES

(1) Friedel L., "Improved friction pressure drop correlations for horizontal and vertical two-phase pipe flow", European Two-Phase Flow Group Meeting, Ispra, 5-8 June 1979, Paper E2.

(2) Petrick M., "A study of carry-under phenomena in vapor liquid separation", A.I.Ch.E. 1963, Volume 9, No. 2, pp.253-260.

(3) Kinghorn F.C. "Two-phase flow measurement using differential pressure meters", Multi-Phase Flow Measurement Course, 1985, London.

(4) Sutton G.W., Hurwitz H., Poritsky H., "Electrical and pressure losses in a magnetohydrodynamic channel due to end current loops", Trans. AIEE, 1961, Part I, Communication and Electronics, pp.687-695.

(5) Baroczy C.J., "Correlation of liquid fraction in two-phase flow with application to liquid metals", Chem. Eng. Progress Symp. Series, 1965, Vol. 61, N.57.

(6) Smissaert G.E., "Two-component two-phase flow parameters for low circulation rates", Report ANL-6755, 1963 Argonne National Laboratory, Il., U.S.A.